

Assessing grapevine water status through fusion of hyperspectral imaging and 3D point clouds



Chenchen Kang^{a,b,d}, Geraldine Diverres^c, Manoj Karkee^{a,b,*}, Qin Zhang^{a,b}, Markus Keller^c

^a Center for Precision and Automated Agricultural Systems, Washington State University, Prosser, WA, USA

^b Department of Biological Systems Engineering, Washington State University, Prosser, WA, USA

^c Department of Viticulture and Enology, Washington State University, Prosser, WA USA

^d Department of Agricultural and Biological Engineering, The Pennsylvania State University, Biglerville, PA USA

ARTICLE INFO

Keywords:

Data fusion
Hyperspectral imaging
3D point cloud
Water stress
Grapevine

ABSTRACT

Mild to moderate and timely water deficit is desirable in grape production to optimize fruit quality for wine-making. It is crucial to develop robust and rapid approaches to assess grapevine water stress for scheduling deficit irrigation. Hyperspectral imaging (HSI) has the potential to detect changes in leaf water status, but the robustness and accuracy are restricted in field applications. The varied leaf orientations can significantly affect how light interacts with the plant, ultimately influencing the reflectance properties. This study focused on developing an approach for detecting grapevine water status using HSI and 3D data. Leaf orientation parameters derived from 3D point clouds were integrated with spectral signatures to address the spectral variance caused by variations in leaf orientation. A water status assessment model was developed based on multiblock partial least squares (MBPLS) to estimate midday leaf water potential (Ψ_L) using spectral signatures and leaf orientation parameters. HSI and 3D point clouds of selected leaves were captured simultaneously in a vineyard during the 2021 growing season, and Ψ_L was measured as the ground truth to assess the model performance. Mean spectral reflectance was derived from the hyperspectral images, while leaf orientation parameters were extracted from 3D point cloud data. The dataset was split randomly into 70% training/calibration and 30% test datasets. The test result shows that the model estimated the Ψ_L with $R^2 = 0.89$, RMSE=0.12 MPa and MAE=0.09 MPa. The leaf orientation parameters derived from 3D point clouds had a contribution of 6.25% in estimating Ψ_L . Moreover, it acted as an enhancing component that explained the spectral variance caused by variations in leaf orientation and improved the interpretation of the underlying relationship between spectral reflectance and vine water status.

1. Introduction

Wine grapes are predominantly cultivated in areas across the globe that experience periodic droughts. In these regions, the rainfall in the summer cannot compensate for the plant water loss through evapotranspiration; and therefore, irrigation is essential to provide sufficient water for plant growth and productivity. The water status at various phenological stages of grapevine growth has significant effects on crop yield, grape composition and quality attributes, which could alter the wine quality (Acevedo-Opazo et al., 2010; Diverres et al., 2024). Over-irrigation may promote excessive shoot growth and canopy density, negatively impacting berry pigments (color) and sugar content, which could lower wine quality (Chaves et al., 2010). Thus, mild to moderate

and timely water deficit is desirable for wine grape production to achieve an appropriate balance between grape yield and quality (Kang et al., 2023b; Martínez-Moreno et al., 2022; Palai et al., 2022).

The efficient management of the water deficit in vines relies on the accurate assessment of grapevine water status. Soil water content measurement, which assesses the trend of available water in the plant root zone, is the most common approach to estimating the plant water status. However, it is time-consuming and costly (limiting the sampling resolution), and introduces great uncertainty in decision-making due to a wide spatial variation in vineyards (Pellegrino et al., 2005). Various physiological characteristics of plants can indicate the reaction of these crops to different degrees of water availability. Therefore, numerous plant-based measures, including sap flow (Escalona et al., 2002),

* Corresponding author at: Center for Precision and Automated Agricultural Systems, Washington State University, USA.

E-mail address: manoj.karkee@wsu.edu (M. Karkee).

stomatal conductance (g_s) (Pirasteh-Anosheh et al., 2016), leaf water potential (Ψ_L), and stem water potential (Ψ_S) (Chone et al., 2001; Reddy et al., 2021) have also been investigated for water status assessment. These measures, however, are destructive to the plants and/or are very time-consuming, and they cannot capture the spatial variability of water status without excessive sampling.

Remote and proximal sensing techniques, such as spectral and thermal sensing, provide opportunities for non-destructive and rapid assessment of grapevine water status (Zhou et al., 2022). Multispectral cameras have been widely used to capture and analyze airborne imagery, which has shown significant correlations between vegetation indices (VIs) and in-situ measurements of plant water status indicators such as g_s and Ψ (Romero et al., 2018). Many studies also used hand-held hyperspectral spectrometers to capture the spectral reflectance of grapevine leaves. In these studies, correlations between several VIs and g_s or Ψ were analyzed (Pócas et al., 2015; Rodríguez-Pérez et al., 2007). These studies demonstrated the potential of hyperspectral sensing for assessing the water status of grapevine. While these spectrometers can only measure reflectance at one canopy location at a time, thus limiting the number of points to be covered, hyperspectral imaging (HSI) systems are significantly quicker at scanning and mapping entire canopy regions and thus facilitating efficient coverage of large vineyard areas (Maybury et al., 2018). Hyperspectral imaging from ground-based platforms within the visible and near-infrared (VNIR) spectral range has facilitated the estimation of grapevine water status at a high spatial resolution, enabling leaf-level analysis. This approach allows for the detection of intra-vine variations in water status, providing a deeper understanding of plant water status dynamics (Kang et al., 2023a). Loggenberg et al. (2018) used a VNIR hyperspectral camera to classify water stress levels with spectral signatures, achieving test accuracy of 83.30% and 80.00% using random forest and extreme gradient boosting machine learning models, respectively. Thapa et al. (2022) evaluated several VIs to classify plant water stress into three levels, achieving accuracy of 73.00% and 70.00% using optimized random forest and artificial neural network models, respectively. Ryckewaert et al. (2022) combined spectral and climate data to estimate g_s and transpiration using regression models, achieving R^2 values of 0.66 and 0.63, respectively.

Despite the promising results of this approach, there are still limitations to its robustness and accuracy. Environmental factors, such as varied leaf orientations, varying sunlight, cloud cover and shadows, can lead to inconsistencies in the captured imagery, especially when the sensing is performed at leaf-level (Liu et al., 2020). Therefore, while this approach shows great potential, it is important to recognize and address these limitations to fully realize its benefits. Among these factors, leaf orientation can significantly affect how light interacts with the plant and ultimately influence the reflectance properties. When light strikes a leaf at an oblique angle or perpendicularly, the leaf reflects more light than when it is parallel to the light. Consequently, quantifying the spectral variance caused by the variation in leaf orientations is important to properly interpret the underlying relationship between spectral reflectance and vine water status. Recent advancements in three-dimensional (3D) imaging technologies, particularly in the use of point clouds, offer an opportunity to enhance the accuracy and efficiency of measuring leaf angle and determining leaf orientation. Numerous studies have employed 3D point cloud data for geometric parameter measurement in a variety of plants, thereby enabling high-throughput plant phenotyping (Xiang et al., 2023). In the realm of plant water status estimation, there has been limited integration of geometric information and spectral signatures. However, such a combination offers an opportunity to address spectral variance caused by variations in leaf orientations and improve the interpretation of the underlying relationship between spectral reflectance and vine water status. In summary, the lighting variability caused by varied leaf orientations limits the accuracy and robustness of estimating vine water status at leaf-level through proximal HSI approaches. To address this problem, this study aimed to verify the hypothesis that the geometric information from 3D point clouds may

explain the variability observed in spectral data due to the differing orientations of leaves; and that the combination of spectral signatures and leaf orientation parameters could improve the interpretation of the complex relationship between spectral reflectance and vine water status. The objective of this study was to combine spectral signatures and geometric information, derived from hyperspectral images and 3D point cloud data, respectively, for the purpose of developing a midday leaf water potential estimation model.

2. Materials and Methods

2.1. Experimental site and design

The experiment was conducted in a vineyard located at the Washington State University research farm near Prosser, WA, USA ($46^{\circ}17'49''N$; $119^{\circ}44'07''W$; elevation 354 m). The own-rooted *Vitis vinifera* L. cv. Riesling vines were planted in 2010 on a 2% south-facing slope in rows oriented in north–south direction with inter- and intra-row spacing of 2.7 m and 1.8 m, respectively. The dominant soil in the vineyard is a Warden silt loam with a heterogeneous depth varying between 0.6 and 1.2 m. The regional climate is categorized as a continental semi-desert with an average annual precipitation of 200 mm. A total of 18 vines were randomly selected and were irrigated to field capacity (soil moisture content ~30%) using drip irrigation at the start of grape ripening (E-L: 34–35). Without additional water applied subsequently, the soil water in the root zone of those plants decreased over the ripening period, introducing a gradient of plant water status on those grapevines. On these experimental vines, two to four individual leaves were selected to acquire hyperspectral images as well as midday leaf water potential, thus generating the dataset with variations in leaf water potential for developing a predictive model.

2.2. Water status and image data acquisition

The data collection was conducted weekly for 4 weeks after the irrigation event (described in Section 2.1) during the 2021 growing season. Each week, experimental data was collected over one or two days, ensuring the inclusion of all 18 vines in the data collection process. During each day of the experiment, between 14:00 and 15:30, 2 to 4 healthy and fully developed leaves were labeled from the west side of the canopy on each vine for the ground truth measurements (Fig. 1). These leaves were chosen based on a random selection from those fulfilling the established criteria for midday Ψ_L measurement, in accordance with the methodology outlined by Smith and Prichard (2003). Although Ψ_L measurements are typically taken near solar noon, an image acquisition window from 14:00 to 15:30 was chosen to ensure optimal sun exposure. This consistent and brief timeframe helped to minimize variations in solar angle and other environmental parameters. A total of 213 leaf samples were collected in this study. A meteorological station operated by Washington State University's AgWeatherNet, located approximately 350 m from the vineyard, provided essential environmental data. This station accurately recorded key meteorological parameters including air temperature, dew point, relative humidity, solar radiation, and wind speed, at 15-minute intervals. The mean values of these parameters, captured during the data collection intervals, are detailed in Table 1.

A VNIR hyperspectral camera (Nano-Hyperspec®, Headwall Photonics, Bolton, MA, USA) and a stereo camera (ZED 2, Stereolabs, CA, USA) were mounted on a ground-based sensing platform to capture the image data (Fig. 2a). The cameras were positioned approximately 1.8 m away from the vine and 1.5 m above ground to aim at the center of the canopy (Fig. 2b). The hyperspectral camera captured images within a spectral range of 400–1000 nm divided into 274 spectral bands (FWHM: 6 nm). The line scanning imager had a spatial resolution of 640 pixels, capturing images with a resolution of $\sim 3200 \times 640$ with a scanning angle of 60° . The exposure time was set between 10–15 ms to maintain



Fig. 1. Healthy, sun-exposed, and fully developed leaves of field-grown Riesling grapevines were tagged for ground-truth variable measurements.

Table 1
The average meteorological parameters in the measurement periods.

Parameters	Air temperature	Dew point	Relative humidity	Solar radiation	Wind speed
Unit	°C	°C	%	W/m ²	m/s
Value	24.67 ± 3.28	7.23 ± 3.60	33.42 ± 7.67	496.84 ± 158.24	2.13 ± 0.82

the imager at approximately 90% of saturation when the imager was focusing on the white reference. The frame speed (ms) was equal to the exposure time, which dictated the scan speed. The angular scan speed was calculated based on frame speed and object distance using FOV Calculator in HyperSpec III, which was the Headwall Photonics software for controlling the hyperspectral imaging system. The angular scan speed ranged from 1.2 to 1.8 degree/s. The white reference and dark reference were captured prior to image acquisition. The stereo camera captured 3D point cloud data with a resolution of 2208 × 1242 within a depth range of 0.3–20 m. The ZED 2 captured data as an SVO file, which incorporated all the necessary metadata for processing, including images, transformations, and both the intrinsic and extrinsic parameters of the camera. After image acquisition, Ψ_L was measured using a pressure chamber (Model 615 D, PMS Instrument Company, Albany, OR, USA).

2.3. Data analysis

All data analysis processes were conducted in Python 3.9 unless otherwise specified.

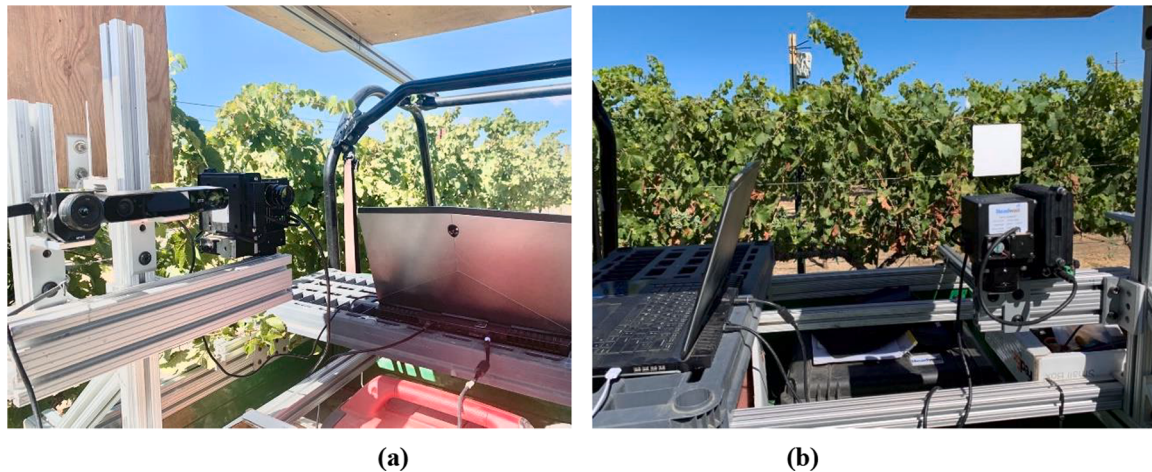


Fig. 2. (a) A VNIR hyperspectral camera and a stereo camera were used to capture the image data; and (b) an overall imaging system where cameras faced the canopy from the west side.

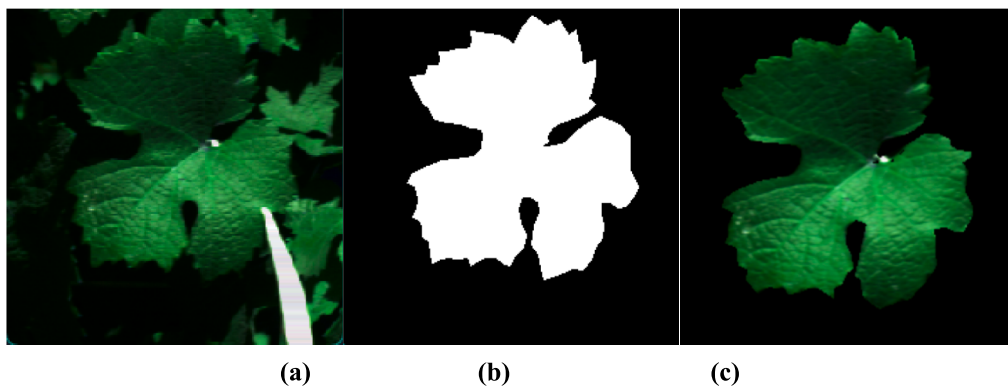


Fig. 3. (a) The labeled leaf was identified by the white tag; (b) a binary mask was created manually; and (c) the leaf area was segmented by the mask.

points belonging to a plane in a 3D point cloud, a distance threshold of 10 mm was set. A plane that had the largest number of points within this distance threshold was selected to represent the leaf orientation. This process returned the plane as an equation $ax + by + cz + d = 0$ in the default 3D coordinate system of the sensor (Fig. 4b). The leaf orientation was denoted by the normal vector n of the fitted plane: $n = [a, b, c]$. For instance, in Fig. 4b, the normal vector of the plane: [0.17, 0.19, 0.97] indicated that the leaf slightly faced south. As the data collection was limited to a fixed period between 14:00 and 15:30, the sun's position and solar angle remained relatively constant during the measurements. Thus, the orientation of the leaves was the main factor affecting the incidence angle of the sun's rays, which in turn influenced the reflectance properties of the leaves.

2.3.3. Data fusion and regression model

Multiblock partial least squares (MBPLS) regression method was employed to combine leaf spectral reflectance and orientation parameters to construct a Ψ_L estimation model. Partial least squares (PLS) regression is commonly used for estimating response variables with

spectral data because of its effectiveness in situations where there are many predictor variables or when the predictor variables are highly correlated (Benelli et al., 2021; Yang et al., 2021). MBPLS is an extension of standard PLS; it divides the multi-source data into different groups according to their conceptual or functional relationships. In MBPLS, the use of conceptually meaningful blocks can provide a more meaningful interpretation of the relationship between the blocks and the output variable (Westerhuis & Smilde, 2001). MBPLS has been commonly used to fuse multi-source data to estimate the output variable due to its interpretability on each block (Baum et al., 2017; Baum & Vermue, 2019). In this study, the reflectance vector: $[r_1, r_2 \dots r_{274}]$ was set as X_1 block and the leaf normal vector: $[a, b, c]$ was set as X_2 block. X_1 and X_2 were used as the inputs of the MBPLS-based model to estimate the output Y variable (Ψ_L).

The dataset was split randomly into 70% training/calibration and 30% test datasets. Leave-one-out cross-validation (LOOCV) was used in the model calibration process to evaluate the model performance with different numbers of latent variables to achieve a minimum mean squared error. The independent 30% dataset was used as the additional test dataset for assessing model performance. Three metrics, coefficient of determination (R^2), root mean square error (RMSE) and mean absolute error (MAE), were used to evaluate model performance. The MBPLS-based model analyzed the underlying relationships between X_1 , X_2 , and Y ; and examined the contribution of each block (X_1 and X_2) to the estimation of Y , measured by the block weight (%). PLSR decomposes the variance in the input variables (X) and the out variables (Y) into a set of latent variables (components). Each component is a linear combination of the original predictor and response variables, where the weights are calculated to maximize the covariance between X and Y (Rosipal and Krämer, 2005). The weights of the blocks (X_1 and X_2) associated with each latent variable, along with the cumulative weights of these blocks (X_1 and X_2) across all latent variables, enable the evaluation of each block's contribution to the estimation of Ψ_L .

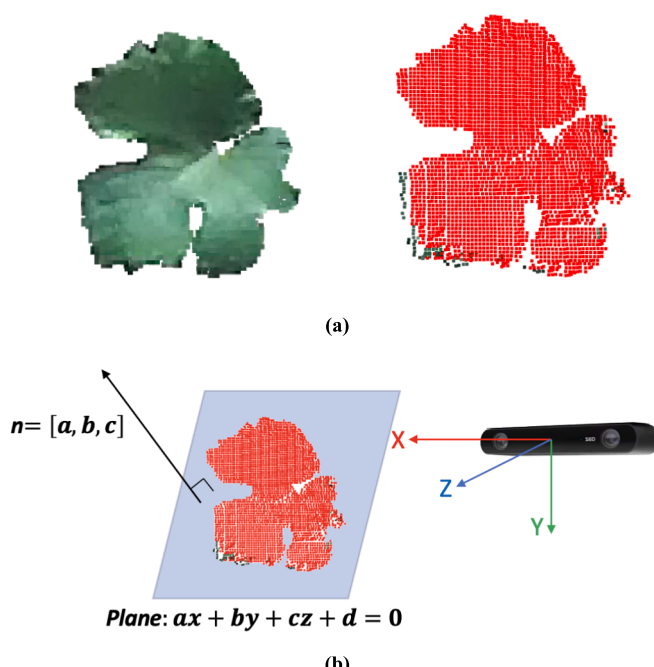


Fig. 4. (a) The tagged leaf was segmented, and a plane was fitted to represent the leaf orientation; (b) RANSAC algorithm returned the plane as $ax + by + cz + d = 0$ in the default 3D coordinate system of the camera. The leaf orientation was denoted by the normal vector of the fitted plane: $n = [a, b, c]$.

3. Results and Discussion

3.1. Data visualization

A total of 213 samples (individual leaves) were collected in this experiment from 18 vines, with each sample consisting of 274 spectral variables (X_1 block), three geometric variables (X_2 block) and one output variable Ψ_L (Y). Fig. 5 (a) shows the distributions of Ψ_L in the datasets. The values of Ψ_L ranged from -1.9 to -0.6 MPa, with the majority of the observations between -1.4 and -0.6 MPa, corresponding to no water stress ($\Psi_L > -0.9$ MPa) and mild to moderate water stress ($-1.4 \text{ MPa} \leq \Psi_L \leq -0.9$ MPa) (Rienht & Scholasch, 2019). A few observations were found between -1.9 and -1.4 MPa, which indicated severe water stress ($\Psi_L < -1.4$ MPa) (Rienht & Scholasch, 2019). The leaf orientations were identified based on their respective normal vectors, which were

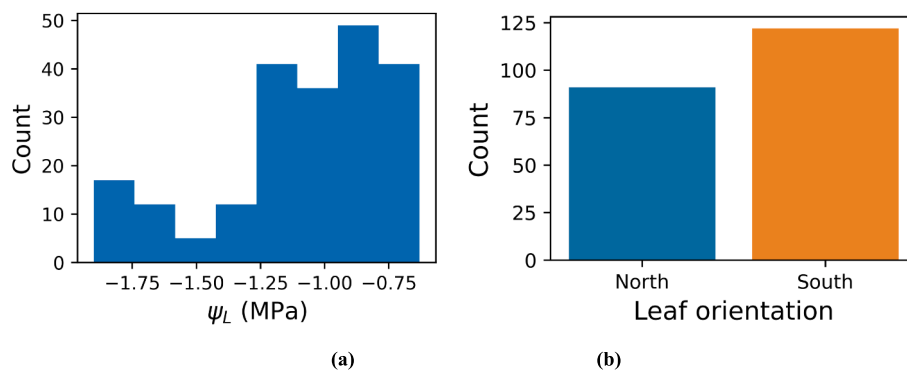


Fig. 5. (a) Histogram of the output variable Ψ_L , displaying the frequency of observations for each value range. (b) Distribution of leaf orientations, displaying the frequency of observations for each orientation group.

subsequently categorized into two groups: those pointing toward the south and those pointing toward the north. Fig. 5(b) presents the distribution of leaf orientations, revealing that a roughly equal number of leaves were observed facing north or south.

The spectral reflectance of vine leaves was found to be influenced by their water status, orientation, and the interactions between these factors. To better understand the spectral variations caused by these factors, the spectra of samples belonging to different stress levels and orientation categories were averaged to obtain a mean observation, and the comparisons were shown in Figs. 6 and 7. Fig. 6 presents the average spectra for each water stress level separately, allowing for a visual representation of the observed differences in spectral patterns. Furthermore, the spectra of samples belonging to two orientation groups were displayed separately. Evident differences in the shape can be found at 550 nm related to leaf pigments and at 700–1000 nm related to leaf structure (Guo et al., 2017; Rapaport et al., 2015; Slaton et al., 2001). The MBPLS model was employed to determine the specific relationship between vine water status and spectral reflectance at each wavelength. Fig. 7 displays the average spectra for two orientation groups, namely south and north, separately. This approach allows for a clear visualization of the observed differences in spectral patterns. Additionally, the spectra of samples belonging to three different water stress levels were also displayed separately. Notably, for each water stress level, leaves facing south exhibited higher reflectance than those facing north. This finding can be attributed to the smaller angles between the leaf plane normal and incident light in the southern orientation. Collectively, the results from Fig. 6 and Fig. 7 emphasize the significance of accounting for both water status and leaf orientation when analyzing spectral reflectance in vine leaves.

3.2. Estimating leaf water potential with an MBPLS-based model

As described in Section 2.3.3, in the model calibration process, different numbers of latent variables/components were investigated to

optimize the model performance using leave-one-out cross-validation, in terms of mean squared error (MSE). Fig. 8 shows the mean squared error curve with increasing number of latent variables. A steep drop was noted when the first five components were engaged in the model, while after five, a slight drop occurred for adding each extra component. The minimum MSE was achieved with 22 latent variables, and MSE started increasing after that.

Fig. 9 presents model-estimated Ψ_L achieved with cross-validation (Fig. 9a) and independent test (Fig. 9b). The green lines correspond to the equation $y = x$, which depicts the perfect/ideal alignment of the estimated Ψ_L with the measured ground truth data. On the other hand, the red lines denote the regression lines relating measured and estimated Ψ_L , which exhibit estimation error and deviations from the ideal relationship. In cross-validation, the model achieved an R^2 of 0.83, indicating that 83% of the variance in the data was explained by the model. The model also demonstrated a low RMSE of 0.14 MPa and MAE of 0.11 MPa, suggesting that the model had good predictive accuracy and low bias. These results indicate that the MBPLS model is capable of accurately estimating Ψ_L from spectral reflectance and leaf orientation parameters of vine leaves. The performance of the model was further evaluated using an independent test dataset, where it achieved an R^2 of 0.89, indicating good agreement between the estimated and measured Ψ_L values. The RMSE of 0.12 MPa and MAE of 0.09 MPa were also relatively low, indicating good predictive accuracy and low bias. The consistency of the model's performance in both cross-validation and independent testing suggests that it is robust and reliable.

Plant water deficits induce physiological changes in leaves, which could be reflected in the electromagnetic spectrum and result in changes in spectral signatures that differ from those of vines receiving an ample water supply (Liu et al., 2020). Additionally, variations in leaf orientations influence the incident light angles on the leaf surfaces, further altering the spectral patterns reflected by the leaves. As discussed in Section 3.1, the spectral reflectance of vine leaves is determined by their water status and orientation, as well as the interactions between these

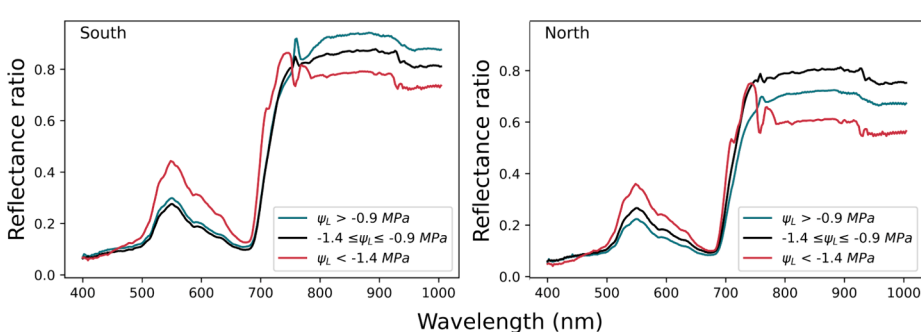


Fig. 6. The spectra were averaged by water stress levels and leaf orientations, providing a visual representation of the observed differences in spectral patterns.

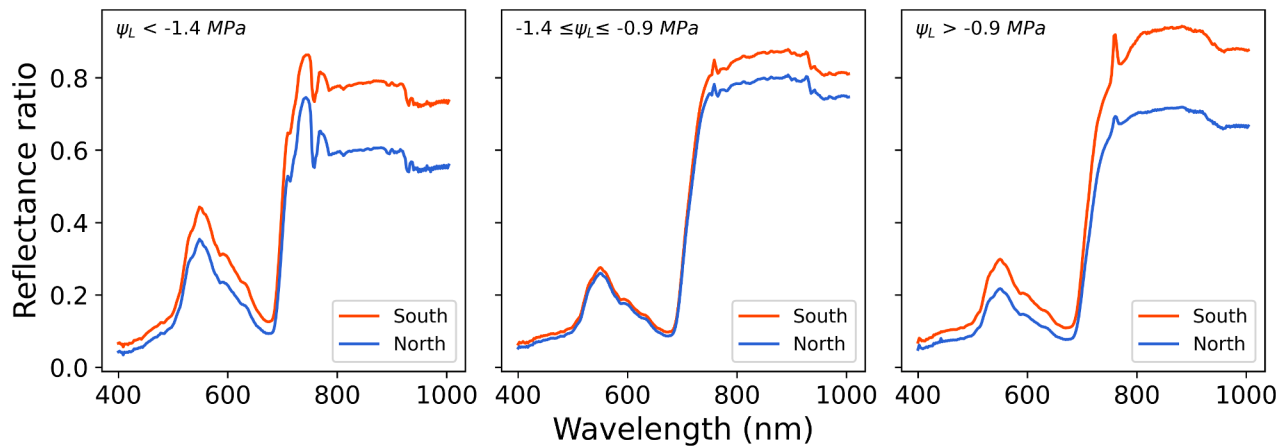


Fig. 7. The spectra were averaged by water stress levels and leaf orientations, providing a visual representation of the observed differences in spectral patterns.

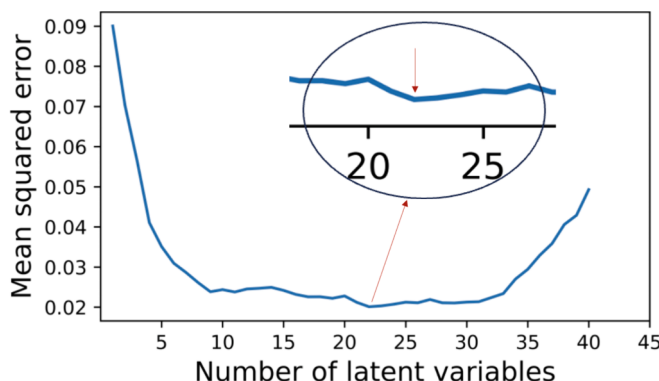


Fig. 8. The minimum mean squared error (MSE) was achieved with 22 latent variables, as indicated by the curve showing MSE variation with different numbers of latent variables.

factors. The MBPLS (Multi-Block Partial Least Squares) regression model was employed to quantify how variations in the spectral data could be attributed to changes in leaf water status and orientation. This model facilitated the development of a predictive model that uses leaf water

status (X_1) and leaf orientation (X_2) to predict leaf water potential (Y). Fig. 10 presents the blocks' weights (X_1 and X_2) for each latent variable, which allows for an assessment of the contribution of each block to the estimation of Ψ_L . The weight values indicate the relative contribution of a particular variable (or group of variables) to the underlying latent variable. In this study, the total weights of leaf orientation variables across all latent variables were found to be 6.25%, suggesting a minor contribution to the estimation of Ψ_L . However, leaf orientation parameters could still be a useful factor in accounting for variations in spectral signatures when multiple leaf samples with similar water status exhibit different spectral characteristics. This nuanced understanding emphasizes the complexity of spectral analysis and underscores the importance of considering multiple biophysical factors in predictive modeling.

Fig. 11a shows the performance of a PLS model using only spectral variables. It was evaluated with the same test dataset as the MBPLS model. Fig. 11b displays the same result as Fig. 9b, providing a basis for comparison. It was noticed that by fusing blocks X_1 and X_2 , the R^2 between estimated and measured values was improved from 0.87 to 0.89, whereas the RMSE was reduced from 0.14 to 0.12 MPa, and the MAE was reduced from 0.11 to 0.09 MPa. These results confirmed the previous analysis on block contribution. The leaf orientation parameters derived from 3D point clouds had a modest contribution to estimating leaf water stress. The high accuracy achieved using only spectral

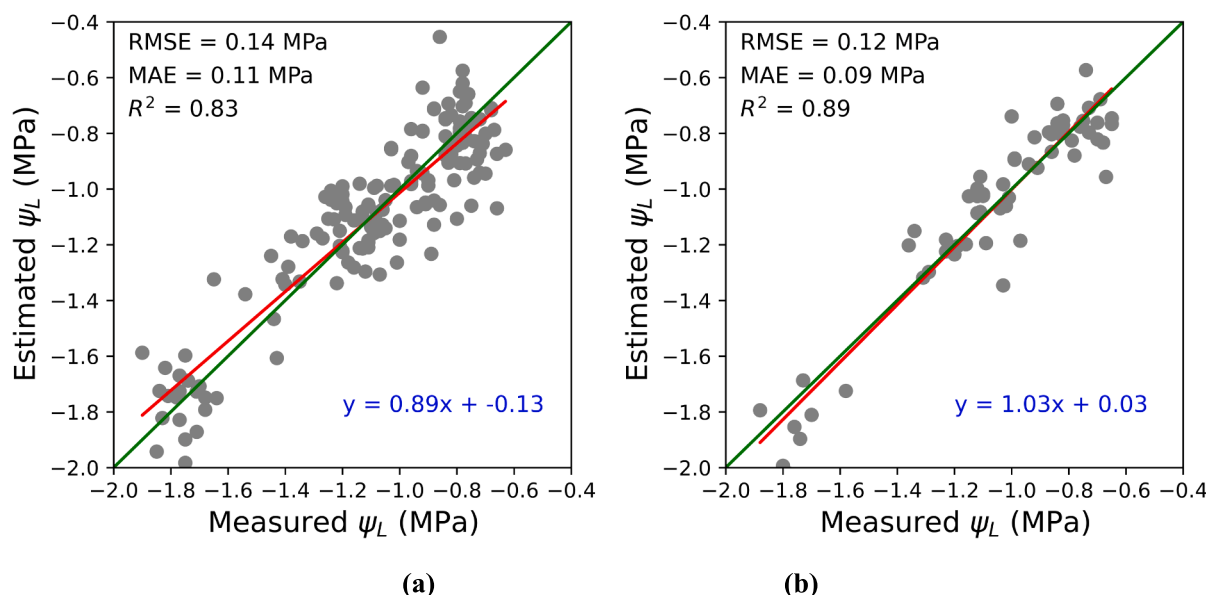


Fig. 9. Performance of the MBPLS model during (a) cross-validation, and (b) testing with the independent dataset.

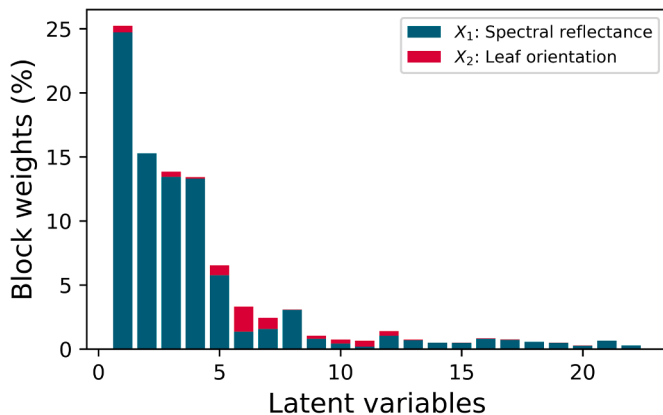


Fig. 10. Blocks' weights across each latent variable indicate the contribution of each block to the estimation of Ψ_L .

variables indicates that most variance in spectral reflectance can be explained by variations in leaf water status. The inclusion of leaf orientation parameters accounted for additional variance in spectral reflectance due to varying leaf orientations, thus clarifying the relationship between spectral reflectance and leaf water status. Although the contribution of leaf orientation is relatively minor, it enhances the model by explaining spectral variance caused by leaf orientation variations, thus improving the interpretation of the relationship between spectral reflectance and vine water status. Collectively, these findings demonstrate the importance of considering multiple factors and data sources when estimating vine water status. Furthermore, this study exemplifies a noteworthy effort towards investigating integrated methodologies for complex modeling within open-field agricultural systems. It also offers a potential solution for other applications, such as estimating grapevine nutrient status. In such cases, where accuracy using only spectral data is low, integrated methodologies might substantially improve predictive accuracy.

While the study offered valuable insights, it is important to acknowledge the potential limitations that may affect the generalizability of the findings. One limitation was that the solar angle still varied since the data collection was conducted over several weeks. To enhance the accuracy and validity of future research, it is recommended to integrate the solar angle into the model to gain a more comprehensive understanding of the intricate interactions between sunlight and plant growth. Additionally, future studies with larger datasets are necessary to evaluate the generalizability and overall performance of the approach.

4. Conclusion

This study was focused on developing an approach for detecting grapevine water status using hyperspectral imagery (HSI) and 3D point cloud data. Leaf orientation parameters derived from 3D point clouds were integrated with spectral signatures to address the spectral variance caused by variations in leaf orientation. A water status assessment model was developed based on Multiblock partial least squares (MBPLS) to estimate leaf water potential (Ψ_L), a measure of plant water status. The following conclusions were drawn based on the results obtained from this study:

- (1) The fusion of spectral signatures and leaf orientation parameters is capable of high-resolution sensing of grapevine water status by estimating Ψ_L at the leaf level. The leaf orientation information can be an enhancing component that explained the spectral variance caused by varying leaf orientation and improved the interpretation of the relationship between spectral reflectance and Ψ_L .
- (2) This study addresses the limitations of traditional spectral analysis caused by the variability in leaf orientations, demonstrating the importance of considering multiple factors and data sources when estimating vine water status. Furthermore, this study exemplifies a noteworthy effort towards investigating integrated methodologies for complex modeling within open-field agricultural systems.

CRediT authorship contribution statement

Chenchen Kang: Writing – original draft, Visualization, Validation, Software, Methodology, Investigation, Formal analysis, Data curation, Conceptualization. **Geraldine Diverres:** Writing – review & editing, Methodology, Investigation, Data curation. **Manoj Karkee:** Writing – review & editing, Supervision, Resources, Methodology, Funding acquisition, Conceptualization. **Qin Zhang:** Writing – review & editing, Supervision, Resources, Methodology, Funding acquisition, Conceptualization. **Markus Keller:** Writing – review & editing, Resources, Methodology, Funding acquisition, Conceptualization.

Declaration of competing interest

The authors declare that they have no known competing financial interests or personal relationships that could have appeared to influence the work reported in this paper.

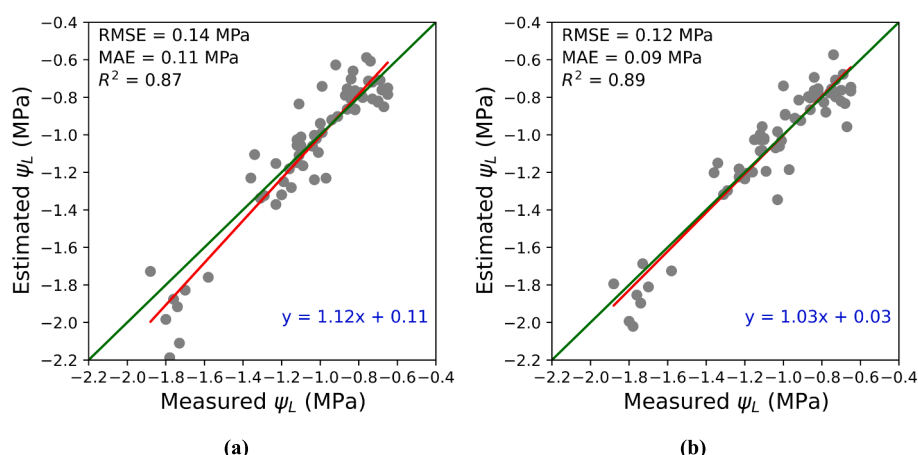


Fig. 11. Comparing model performance on a test dataset for the estimation of Ψ_L using (a) spectral variables and (b) spectral and leaf orientation variables.

Data availability

Data will be made available on request.

Acknowledgements

This research was supported by the U.S. Department of Agriculture's National Institute of Food and Agriculture (USDA NIFA; accession no. 1005756). All authors would like to thank Patrick A Scharf and Alan Kawakami for their skilled technical assistance.

References

- Acevedo-Opazo, C., Ortega-Farias, S., Fuentes, S., 2010. Effects of grapevine (*Vitis vinifera* L.) water status on water consumption, vegetative growth and grape quality: An irrigation scheduling application to achieve regulated deficit irrigation. *Agric. Water Manag.* 97 (7), 956–964.
- Baum, A., Dominiak, M., Vidal-Melgosa, S., Willats, W.G., Søndergaard, K.M., Hansen, P.W., Meyer, A.S., Mikkelsen, J.D., 2017. Prediction of pectin yield and quality by FTIR and carbohydrate microarray analysis. *Food Bioproc. Tech.* 10 (1), 143–154.
- Baum, A., Vermue, L., 2019. Multiblock PLS: Block dependent prediction modeling for Python. *J. Open Source Software* 4 (34), 1190.
- Benelli, A., Cevoli, C., Ragni, L., Fabbri, A., 2021. In-field and non-destructive monitoring of grapes maturity by hyperspectral imaging. *Biosyst. Eng.* 207, 59–67.
- Chaves, M.M., Zarrouk, O., Francisco, R., Costa, J.M., Santos, T., Regalado, A.P., Rodrigues, M.L., Lopes, C.M., 2010. Grapevine under deficit irrigation: hints from physiological and molecular data. *Ann. Bot.* 105 (5), 661–676.
- Chone, X., Van Leeuwen, C., Dubourdieu, D., Gaudillère, J.P., 2001. Stem water potential is a sensitive indicator of grapevine water status. *Ann. Bot.* 87 (4), 477–483.
- Diverres, G., Fox, D.J., Harbortson, J.F., Karkee, M., Keller, M., 2024. Response of riesling grapes and wine to temporally and spatially heterogeneous soil water availability. *Am. J. Enol. Vitic.* 75 (2).
- Escalona, J., Flexas, J., Medrano, H., 2002. Drought effects on water flow, photosynthesis and growth of potted grapevines. *VITIS-Geilweilerhof* 41 (2), 57–62.
- Guo, J.-T., Yang, D.-C., Guan, Z., He, Y.-H., 2017. Chlorophyll-catalyzed visible-light-mediated synthesis of tetrahydroquinolines from N, N-dimethylanilines and maleimides. *J. Org. Chem.* 82 (4), 1888–1894.
- Kang, C., Diverres, G., Achyut, P., Karkee, M., Zhang, Q., Keller, M., 2023a. Estimating soil and grapevine water status using ground based hyperspectral imaging under diffused lighting conditions: Addressing the effect of lighting variability in vineyards. *Comput. Electron. Agric.* 212, 108175.
- Kang, C., Diverres, G., Karkee, M., Zhang, Q., Keller, M., 2023b. Decision-support system for precision regulated deficit irrigation management for wine grapes. *Comput. Electron. Agric.* 208.
- Liu, H., Bruning, B., Garnett, T., Berger, B., 2020. Hyperspectral imaging and 3D technologies for plant phenotyping: From satellite to close-range sensing. *Comput. Electron. Agric.* 175.
- Loggenberg, K., Strever, A., Greylings, B., Poona, N., 2018. Modelling water stress in a shiraz vineyard using hyperspectral imaging and machine learning. *Remote Sens. (Basel)* 10 (2).
- Lu, Y., Li, X., Young, S., Li, X., Linder, E., Suchoff, D., 2022. Hyperspectral imaging with chemometrics for non-destructive determination of cannabinoids in floral and leaf materials of industrial hemp (*Cannabis sativa* L.). *Comput. Electron. Agric.* 202.
- Martínez-Moreno, A., Pérez-Alvarez, E.P., Intrigliolo, D.S., Mirás-Avalos, J.M., López-Urrea, R., Gil-Muñoz, R., Lizama, V., García-Esparza, M.J., Álvarez, M.I., Buesa, I., 2022. Effects of deficit irrigation with saline water on yield and grape composition of *Vitis vinifera* L. cv. Monastrell. *Irrigation Science*.
- Maybury, I.J., Howell, D., Terras, M., Viles, H., 2018. Comparing the effectiveness of hyperspectral imaging and Raman spectroscopy: a case study on Armenian manuscripts. *Heritage Sci.* 6 (1), 42.
- Palai, G., Caruso, G., Gucci, R., D'Onofrio, C., 2022. Deficit irrigation differently affects aroma composition in berries of *Vitis vinifera* L. (cvS Sangiovese and Merlot) grafted on two rootstocks. *Aust. J. Grape Wine Res.* 28 (4), 590–606.
- Pellegrino, A., Lebon, E., Simonneau, T., Wery, J., 2005. Towards a simple indicator of water stress in grapevine (*Vitis vinifera* L.) based on the differential sensitivities of vegetative growth components. *Aust. J. Grape Wine Res.* 11 (3), 306–315.
- Pirasteh-Anosheh, H., Saeed-Mousheshi, A., Pakniyat, H., Pessarakli, M., 2016. Stomatal responses to drought stress. *Water Stress and Crop Plants* 24–40.
- Poças, I., Rodrigues, A., Gonçalves, S., Costa, P., Gonçalves, I., Pereira, L., Cunha, M., 2015. Predicting grapevine water status based on hyperspectral reflectance vegetation indices. *Remote Sens. (Basel)* 7 (12), 16460–16479.
- Rapaport, T., Hochberg, U., Shoshany, M., Karniel, A., Rachmievitch, S., 2015. Combining leaf physiology, hyperspectral imaging and partial least squares-regression (PLS-R) for grapevine water status assessment. *ISPRS J. Photogramm. Remote Sens.* 109, 88–97.
- Reddy, Y.A.N., Reddy, Y.N.P., Ramya, V., Suma, L.S., Reddy, A.B.N., Krishna, S.S., 2021. Chapter 8 - Drought adaptation: Approaches for crop improvement. In: Singh, M., Sood, S. (Eds.), *Millets and Pseudo Cereals*. Woodhead Publishing, pp. 143–158.
- Rienth, M., Scholasch, T., 2019. State-of-the-art of tools and methods to assess vine water status. *OENO One* 53 (4).
- Rodríguez-Pérez, J.R., Riaño, D., Carlisle, E., Ustin, S., Smart, D.R., 2007. Evaluation of hyperspectral reflectance indexes to detect grapevine water status in vineyards. *Am. J. Enol. Vitic.* 58 (3), 302–317.
- Romero, M., Luo, Y., Su, B., Fuentes, S., 2018. Vineyard water status estimation using multispectral imagery from an UAV platform and machine learning algorithms for irrigation scheduling management. *Comput. Electron. Agric.* 147, 109–117.
- Rosipal, R., Krämer, N., 2005. Overview and recent advances in partial least squares. In: *In International Statistical and Optimization Perspectives Workshop "Subspace, Latent Structure and Feature Selection"*. Springer Berlin Heidelberg, Berlin, Heidelberg, pp. 34–51.
- Ryckewaert, M., Héran, D., Simonneau, T., Abdelghafoor, F., Boulord, R., Saurin, N., Moura, D., Mas-Garcia, S., Bendoula, R., 2022. Physiological primary predictions using VIS-NIR spectroscopy for water stress detection on grapevine: Interest in combining climate data using multiblock method. *Comput. Electron. Agric.* 197.
- Slaton, M.R., Raymond Hunt Jr, E., Smith, W.K., 2001. Estimating near-infrared leaf reflectance from leaf structural characteristics. *Am. J. Bot.* 88 (2), 278–284.
- Smith, R., & Prichard, T. (2003, July). Using a Pressure Chamber in Winegrapes. <https://ucanr.edu/sites/SoCo/files/27409.pdf>.
- Thapa, S., Kang, C., Diverres, G., Karkee, M., Zhang, Q., Keller, M., 2022. Assessment of water stress in vineyards using on-the-go hyperspectral imaging and machine learning algorithms. *J. ASABE* 65 (5), 949–962.
- Westerhuis, J.A., Smilde, A.K., 2001. Deflation in multiblock PLS. *J. Chemom.* 15 (5), 485–493.
- Xiang, L., Gai, J., Bao, Y., Yu, J., Schnabel, P.S., Tang, L., 2023. Field-based robotic leaf angle detection and characterization of maize plants using stereo vision and deep convolutional neural networks. *J. Field Rob.*
- Yang, Y., Wang, W., Zhuang, H., Yoon, S.C., Jiang, H., 2021. Prediction of quality traits and grades of intact chicken breast fillets by hyperspectral imaging. *Br Poult Sci* 62 (1), 46–52.
- Zhou, Z., Diverres, G., Kang, C., Thapa, S., Karkee, M., Zhang, Q., Keller, M., 2022. Ground-based thermal imaging for assessing crop water status in grapevines over a growing season. *Agronomy* 12 (2), 322.
- Zhou, Q.-Y., Park, J., & Koltun, V. (2018). Open3D: A modern library for 3D data processing. *arXiv preprint arXiv:1801.09847*.